DOI: 10.1021/ma900820g

Macromolecules
ARTICLE

Gelation Mechanism of Thermoreversible Supramacromolecular Ion Gels via Hydrogen Bonding

Atsushi Noro,*,† Yushu Matsushita,† and Timothy P. Lodge*,‡,§

†*Department of Applied Chemistry, Graduate School of Engineering, Nagoya University, Furo-cho, Chikusa-ku, Nagoya 464-8603, Japan,* ‡*Department of Chemistry, University of Minnesota, 207 Pleasant Street SE, Minneapolis, Minnesota 55455, and* §*Department of Chemical Engineering & Materials Science, University of Minnesota, 421 Washington Avenue SE, Minneapolis, Minnesota 55455*

Received April 15, 2009; Revised Manuscript Received June 2, 2009

ABSTRACT: A series of supramacromolecular ion gels were prepared from blends of a poly(2-vinylpyridine)-*b*-poly(ethyl acrylate)-*b*-poly(2-vinylpyridine) (VEAV) triblock copolymer and a poly(4-hydroxystyrene) (H) homopolymer in an ionic liquid. The VEAV concentration was held at 10 wt %, and the H concentration was varied from 0 to 8 wt %. The solvent was the room temperature ionic liquid 1-ethyl-3-methylimidazolium bis(trifluoromethylsulfonyl) imide (EMITFSI). Above 160 °C all samples formed homogeneous solutions, but upon cooling gels were formed due to increased hydrogen bonds between the V blocks and H cross-linkers. The gelation mechanism was investigated in detail by rheology and small-angle X-ray scattering. The gel point (gel−liquid transition temperature) increased with the concentration of the cross-linkers. The dynamic moduli, G' and G'', showed excellent time−temperature superposition, and gave master curves extending over 15 orders of magnitude in reduced frequency. The shift factors a_T showed the same strong temperature dependence for all the samples, which is attributed to the increasing number of hydrogen bonds between a given V block and H cross-linker upon cooling below the gel point. The gel quality was assessed in terms of the modulus value, G_x, the sharpness of the change in dynamic moduli with temperature near the gel point, and the minimum value of tan δ in the gel regime. By all three measures the best gel was formed at the mole ratio closest to 1:1 of pyridine:phenol units, *i.e.*, stoichiometric balance. Furthermore, the maximum value of G_x corresponded to 50% of the EA blocks being elastically effective, consistent with expectation given the tendency for midblocks to loop back into the same micelle. A gel-like response was also obtained upon mixing 10% of a poly(2-vinylpyridine)-*b*-poly(ethyl acrylate) (VEA) diblock copolymer and H homopolymers in EMITFSI. However, in this case the rheological properties resulted from congestion of micelles rather than bridging chains. Small angle X-ray scattering revealed the presence of a nanophase-separated state, but without any significant change on traversing the gel point, or between diblock and triblock samples.

Introduction

Supramolecular interactions, such as hydrogen bonding,[1−3] ionic interactions,[4−6] and others[7−9] have been widely explored in macromolecular science,[10] from both fundamental and applied viewpoints. Such interactions have attracted increasing attention to produce a variety of self-healing[11] and stimuli-responsive materials.[12] They are also useful to study complexation of materials,[13−16] new nanostructure construction,[17−26] and control of viscoelastic properties.[27−32] Although supramolecular interactions represent very interesting approaches for many studies in macromolecular science,[33−36] there are some practical difficulties. Because of the glass transition and entanglement the mobility of macromolecules in bulk is limited, and it may be difficult to achieve a rapid response by association−dissociation or switching of supramolecular interactions in macromolecular complexes. If solvents are used as media for macromolecules, the mobility can be greatly enhanced. However, organic solvents or water are volatile, and this is unfavorable especially for temperature-responsive supramolecular materials.

Recently, we have described thermoreversible "supramacromolecular ion gels",[37] made from hydrogen-bonded supramacromolecules in an ionic liquid, where the term supramacromolecule denotes supramolecular assembly composed of macromolecules. Two component macromolecules were blended in an ionic liquid: an ionic-liquid soluble ABA triblock copolymer with poly(2-vinylpyridine) (V) end blocks and a poly(ethyl acrylate) (EA) midblock, and a poly(4-hydroxystyrene) (H) homopolymer, such that hydrogen bonding results between the pyridine and phenol units.[38−40] Ionic liquids (ILs) solvents have many attractive properties such as negligible volatility, nonflammability, and thermal stability,[41−43] which render them promising media for macromolecular studies,[44−49] and which provide multiple opportunities for macromolecular materials.[50,51] As an example, ion gels,[52−56] which are polymeric networks swollen with ionic liquids, have been considered for various applications including actuators, gas separation membranes, organic thin-film transistors, and lithium batteries.[57−62] In a previous paper,[37] we exploited an ionic liquid as a negligibly volatile and thermally stable medium for thermoreversible supramacromolecules. Among the most striking features of the results was the formation of a thermoreversible ion gel, with a longest relaxation time that varied by over 11 orders of magnitude on cooling to room temperature from the gel point near 140 °C.

Here we further explore the gelation mechanism for supramacromolecular ion gels made from poly(2-vinylpyridine)-*b*-poly(ethyl acrylate)-*b*-poly(2-vinylpyridine) (VEAV) triblock copolymer/poly(4-hydroxystyrene) (H) blends, with varying amounts of H as hydrogen bonding cross-linkers, in the ionic liquid 1-ethyl-3-methylimidazolium bis(trifluoromethylsulfonyl) imide (EMITFSI). The samples were characterized by rheology

*Corresponding authors. E-mail: (A.N.) noro@nagoya-u.jp; (T.P.L.) lodge@umn.edu.

 Published on Web 06/24/2009

Table 1. Molecular Characteristics of Polymers

sample	M_n[a]	mole fractions[b]	PDI[c]	DP[d]
VEAV	50000	0.10/0.80/0.10	1.6	50/395/50
VEA	29000	0.23/0.77	1.4	65/220
H	6600		1.09	55

[a] Number average molecular weight. [b] Mole fractions of V/EA/V (or V/EA). [c] Polydispersity index. [d] Degree of polymerization.

and small-angle X-ray scattering. We also prepared a similar sample from a poly(2-vinylpyridine)-*b*-poly(ethyl acrylate) (VEA) diblock copolymer/poly(4-hydroxystyrene) (H) /EMITFSI to compare the response of triblock and diblock systems.

Experimental Section

A poly(2-vinylpyridine)-*b*-poly(ethyl acrylate)-*b*-poly(2-vinylpyridine) triblock copolymer (VEAV), a poly(2-vinylpyridine)-*b*-poly(ethyl acrylate) diblock copolymer (VEA), and a poly(4-hydroxylstyrene) homopolymer (H) were synthesized via reversible addition−fragmentation chain transfer (RAFT) polymerization.[63−66] Synthesis details for VEAV and H were described previously;[37] VEA was synthesized to have approximately half the molecular weight but the same composition as the VEAV triblock copolymer by using the monofunctional chain transfer agent (CTA) S-1-dodecyl-S'(α,α'-dimethyl-α"-acetic acid) trithiocarbonate, with almost the same synthesis conditions as for VEAV. (See also Scheme SI in Supporting Information.) All polymers were purified by multiple reprecipitation.

These polymers were characterized by size exclusion chromatography (SEC) and ^{1}H NMR spectroscopy. The polydispersity indices (PDIs) of the polymers were determined by using three Phenogel columns (Phenomenex) combined with an Alltech 426 HPLC pump and DAWN DSP interferometric reflectometer (Wyatt Technology Corporation) with polystyrene standards. The molecular weight of the H homopolymer was determined by ^{1}H NMR (Varian) by end-group analysis.[67] The mole fractions of the blocks in the VEAV triblock copolymer and the VEA diblock copolymer were also determined by ^{1}H NMR. For the VEAV triblock copolymer, the total number-average molecular weight (M_n), polydispersity index (PDI), and mole fractions of V/EA/V were determined to be 50 000, 1.6, and 0.10/0.80/0.10, respectively. For the VEA diblock copolymer, M_n, PDI, and mole fractions of V/EA were determined to be 29 000, 1.4, and 0.23/0.77. For the H homopolymer, M_n and PDI were determined to be 6600 and 1.09, respectively. Table 1 summarizes the characterization results.

The hydrophobic and thermally stable ionic liquid (IL) 1-ethyl-3-methylimidazolium bis(trifluoromethylsulfonyl) imide (EMITFSI)[68,69] was used as a solvent. The same preparation method with tetrahydrofuran (THF) as a volatile cosolvent was used as reported previously.[37] To investigate the effect of the concentration of the H homopolymer, *i.e.*, the number of available hydrogen bond donors, IL solutions were prepared by changing the weight ratios of VEAV/H at constant VEAV concentration. Five blend solutions and a solution of a pure triblock copolymer were prepared, that is, t-10/0, t-10/0.5, t-10/1, t-10/2, t-10/4, and t-10/8. To compare the difference between a solution containing triblock copolymers and a solution containing diblock copolymers, an IL solution of VEA/H was prepared with a weight ratio of 10/4, and is coded as d-10/4. Table 2 lists the weight ratios of VEAV/H/IL and VEA/H/IL, mole ratios of block copolymer/ homopolymer, and mole ratios of pyridine units on V to phenol units on H.

Oscillatory shear measurements were performed on an ARES Rheometer (TA Instruments). Dynamic strain sweeps were run to assess the linear viscoelastic regime before each dynamic measurement. Except where noted, all other dynamic tests were obtained in the linear regime. Dynamic temperature ramp tests were run from higher to lower temperature at a ramp rate of 1 °C/min, a strain of 3% or 5%, and a frequency of 0.3 rad/s. Dynamic frequency sweeps were also obtained at ten degree intervals from higher to lower temperatures, and a strain of 3% or 5%.

Table 2. Codes and Characteristics of Blend Samples

code	$W_{VEAV(VEA)}/W_H/W_{IL}$[a]	$X_{VEAV\ (VEA)}/X_H$[b]	$X_{pyridine}/X_{phenol}$[c]	T_{gel}[d]/°C	$D_{cylinder}$[e]/nm
t-10/0	10/0/90	1/0	100/0		
t-10/0.5	10/0.5/90	1/0.38	100/21		
t-10/1	10/1/90	1/0.75	100/41	115	40
t-10/2	10/2/90	1/1.5	100/82	131	35
t-10/4	10/4/90	1/3	100/165	141	34
t-10/8	10/8/90	1/6	100/330	161	32
d-10/4	10/4/90	1/1.8	65/100	148	33

[a] Weight ratio of VEAV(VEA)/H/IL. [b] Mole ratio of VEAV(VEA)/H polymers. [c] Mole ratio of pyridine to phenol units. [d] Gel point determined as the intersection of G' and G'' in Figure 1. [e] Domain spacing between cylinders at room temperature from Figure 4.

To investigate the morphology of cross-linked supramacromolecules in ILs,[70] small-angle X-ray scattering (SAXS) measurements were taken at the beamline 15 A in the Photon Factory, Tsukuba, Japan. The wavelength of the incident X-rays was 0.15 nm, and the camera length was 2.38 m; imaging plates were used as detectors. Samples (gels or solutions) were held between polyimide films and the samples were exposed to the incident beam for the same time (60 s). Temperature control was achieved by using a homemade heater with a temperature controller.

Results

In the previous paper, we documented the striking thermosensitive viscoelastic properties of a supramacromolecular ion gel equivalent to sample t-10/4, with the longest relaxation time increasing by more than 11 orders of magnitude on cooling from the above the gel point at 141.5 °C to room temperature.[37] The gelation itself was attributed to hydrogen bonding between the end blocks of the VEAV triblock copolymer and the H homopolymer. The temperature dependence of the hydrogen bonding was also estimated via FT-IR measurements. In this report, we explore the gelation mechanism in more detail via rheological and SAXS measurements for several samples with different H homopolymer concentrations. In particular, the dependence of the gelation temperature and the quality of the resulting gel on the amount of H cross-linker are examined in detail. We also compare the properties of a solution containing a diblock copolymer in place of the triblock, to establish the role of bridging chains in the gel viscoelasticity.

Oscillatory Shear Measurements. Figure 1 shows dynamic temperature ramp tests for five blend solutions. In Figure 1a, the storage modulus G' for t-10/1 is less than the loss modulus G'' at high temperatures, which indicates liquid-like behavior; G' and G'' intersect at 115 °C. At lower temperatures, $G' > G''$ and both moduli increase with decreasing temperature. Following the previous report,[37] 115 °C can be assigned as the gel point for this sample. Liquid-like behavior is observed at elevated temperatures for t-10/2, t-10/4, and t-10/8 in Figure 1, parts b, c, and d, respectively, but these three samples show higher gel points of 131, 141, and 161 °C, respectively. As for t-10/4, G' reaches a plateau in the modulus (G_x) of 2570 Pa at 30 °C with decreasing temperature below the gel point, with a wide interval of almost temperature independent modulus (actually G' increases slightly, proportional to k_BT. See also the eq 2 in the Discussion). This result indicates that a well-defined network structure has been formed, which is invariant to changes in temperature. The lower temperature values of G' for t-10/2 and t-10/8 are approaching this same plateau value, but are still increasing slightly on cooling, suggesting that the network structure is still evolving. In contrast, although a sample of d-10/4 in Figure 1e shows a gel point of 148 °C, its G' is smaller and G'' is distinctly larger than for all the triblock samples. As will be discussed subsequently,

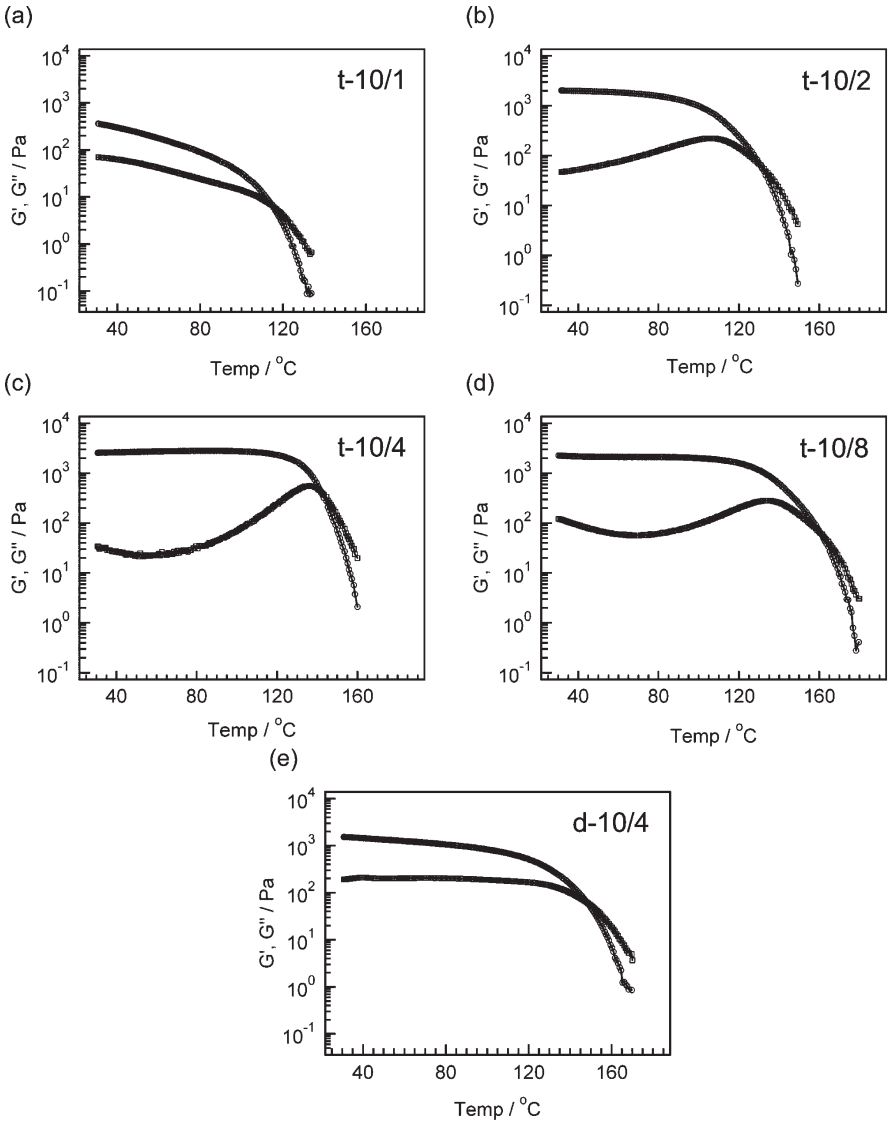

Figure 1. Dynamic moduli G' (○) and G'' (□) vs temperature: (a) t-10/1; (b) t-10/2; (c) t-10/4; (d) t-10/8; (e) d-10/4. All the measurements were performed with the same frequency of 0.3 rad/s. The strain is 3% for t-10/4 and t-10/8 and 5% for t-10/1, t-10/2, and d-10/4.

we attribute the apparent gel-like behavior of the diblock sample to congestion of micelle-like aggregates, rather than the formation of a percolating network.

Dynamic frequency sweeps for the same five samples were also obtained at ten degree intervals from high to low temperature. Time−temperature superposition (TTS) was attempted, and Figure 2 shows double logarithmic master curves for G' and G'' versus reduced frequency ωa_T for all five samples. A single reference temperature of 120 °C was adopted for all samples. TTS works well over a wide temperature range for all the samples, and the reduced frequency axis extends up to 14 orders of magnitude. There are systematic deviations from TTS in G'' at higher frequencies and lower temperatures, which are due to relaxation of the network strands, *i.e.*, the EA blocks. As noted previously,[37] these upturns in G'' may themselves be superposed by shifting the data according to the temperature dependence of the solvent viscosity (see Figures S15 and S16 in Supporting Information). Figure 3 shows the resulting shift factors a_T from Figure 2 as functions of temperature, where a_T denotes the ratio of any relaxation time at one temperature to its value at the chosen reference temperature, 120 °C. The shift factors for the four triblock samples overlap well, whereas those for the diblock have a much weaker temperature dependence below about 100 °C. This is further evidence that the rheological response of the diblock system reflects a different underlying mechanism. Terminal behavior is seen at low reduced frequencies for all five master curves in Figure 2. However, at higher frequencies than the inverse longest relaxation time (taken where $G' = G''$), the behavior of G' and G'' differs among the samples. As noted in Figure 1, there is no plateau in G' for t-10/1, and the same is true in Figure 2a. On the other hand, G' of t-10/4 in Figure 2c reached a plateau modulus, G_x, at higher frequencies and showed the sharpest transition into a very wide plateau, while G' of t-10/2 and t-10/8 in parts b and d of Figure 2 are approaching G_x. Master curves of G' and G'' for d-10/4 are also shown in Figure 2e but do not show a distinct plateau, and also show a larger G'' than the others, as noted in Figure 1.

Small Angle X-ray Scattering. Small angle X-ray scattering (SAXS) experiments were performed for all seven samples to assess the sample structure. SAXS profiles for the seven samples at 30 °C are shown in Figure 4. The vertical axis represents logarithmic intensity, while the horizontal axis represents the scattering wavevector q ($=4\pi(\sin\theta)/\lambda$),

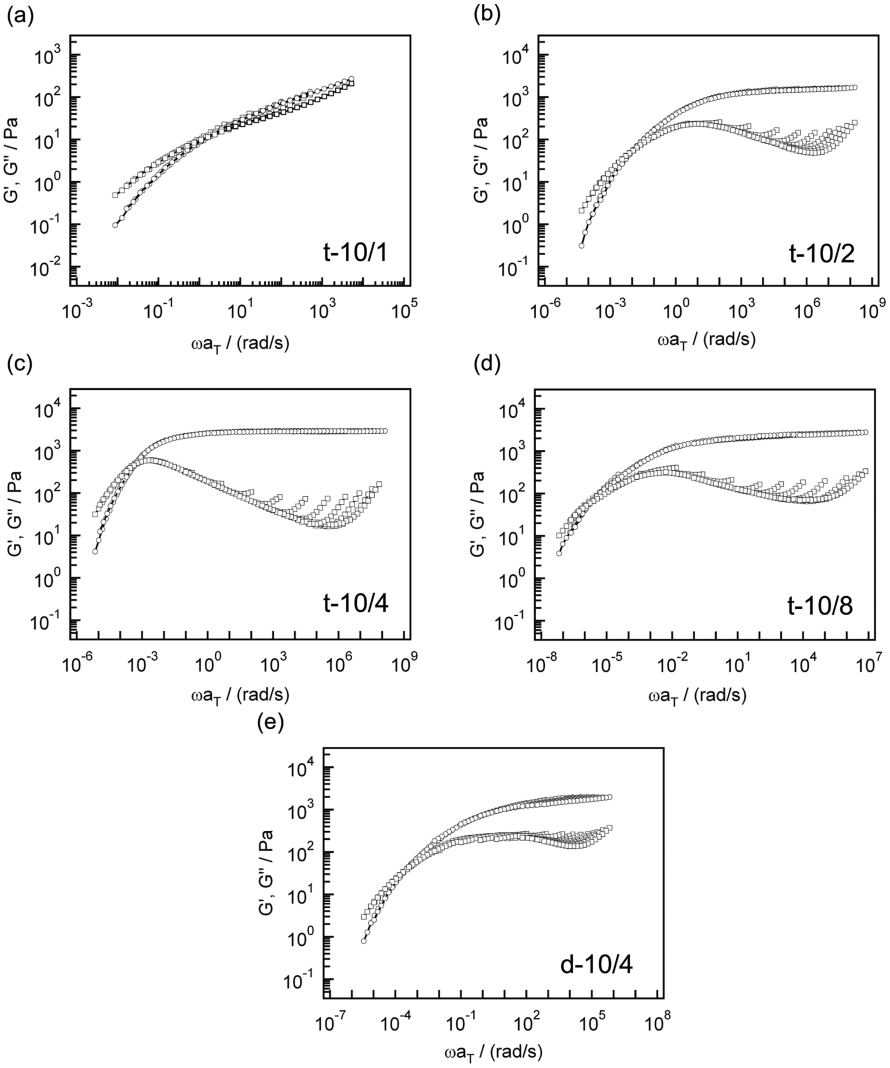

Figure 2. TTS master curves for G' (○) and G'' (□) with a reference temperature of 120 °C: (a) t-10/1; (b) t-10/2; (c) t-10/4; (d) t-10/8; (e) d-10/4.

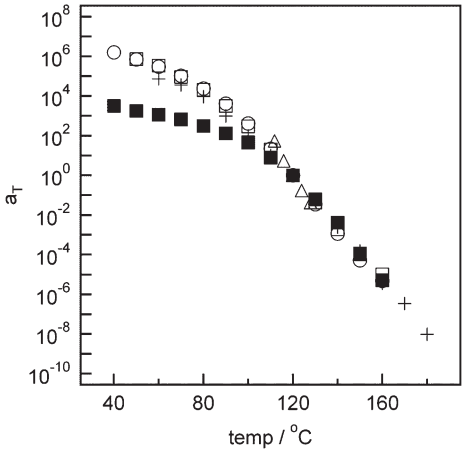

Figure 3. Shift factors for TTS master curves of Figure 2: d-10/4 (■), t-10/1 (△), t-10/2 (○),t-10/4 (□), t-10/8 (+).

where λ and 2θ are the wavelength of X-rays and the scattering angle, respectively. The profiles are displayed in the order of weight ratios from top to bottom, *i.e.*, t-10/8, t-10/4, t-10/2, t-10/1, t-10/0.5, and t-10/0 with d-10/4 at the bottom. The sample of t-10/0 has no peak in Figure 4, indicating that there is no particular nanostructure present,

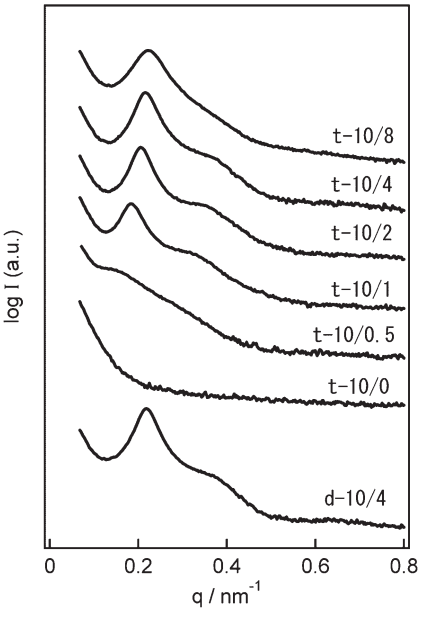

Figure 4. Comparison of SAXS diffraction patterns for different samples at 30 °C. The profiles for t-10/ 8, t-10/4, t-10/2, t-10/1, t-10/0.5, t-10/0, and d-10/4 are displayed from top to bottom.

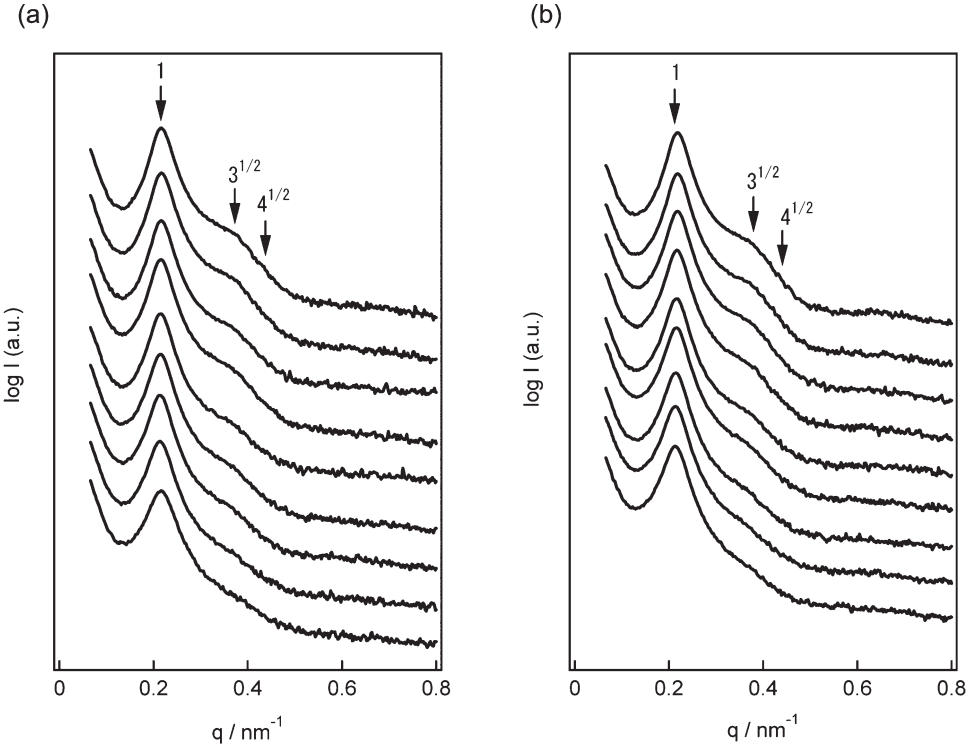

Figure 5. Comparison of SAXS diffraction patterns with different temperatures: (a) t-10/4; (b) d-10/4. The temperatures used are 30, 40, 60, 80, 100, 120, 140, 160, and 180 °C, and profiles are displayed in the same order of temperatures from top to bottom.

as expected. All of the other samples reveal distinct primary peaks, although for t-10/0.5 it is quite broad. We conclude that the addition of homopolymer H induces nanophase separation in these IL solutions, presumably due to hydrogen bonding between H and V. The solutions containing 1% or more H show a shoulder that is consistent with the possibility of underlying higher order reflections at relative q values of $3^{1/2}$ and $4^{1/2}$, which is suggestive of hexagonally packed cylinders. We tentatively attribute this to nanophase-separated V + H associations within a well-solvated EA phase. The location of the first peak shifts to higher q values with increasing amounts of H, that is, the average domain spacing decreases. Assuming an approximately cylindrical structure, the average distance between cylinders for samples was estimated as $D \approx (2/3^{1/2})q_1/2\pi$, and the calculated values are listed in Table 2. Temperature-controlled SAXS experiments were also carried out for t-10/4 and d-10/4. Nine temperatures were used for the experiments: 30, 40, 60, 80, 100, 120, 140, 160, and 180 °C. Figure 5 displays the results, with this sequence of temperatures from top to bottom. The most important aspect of these data is that the triblock and diblock give very similar results, even though the rheological profiles are quite different. This is consistent with expectation that the nanophase structure is dictated primarily by sample composition, whereas the rheology is dominated by the network connectivity (or absence thereof). Also, as will be discussed subsequently, there is no obvious change in the sharpness or height of the primary peaks near the rheological gel point.

Discussion

Relationship between Gelation and Concentration of Hydrogen Bonding Cross-Linkers. It is clear from Figures 1 and 2 that the samples t-10/2, t-10/4, and t-10/8 all form thermoreversible supramacromolecular ion gels with well-defined gel points (where $G' = G''$) and plateau moduli. The gel temperatures increase monotonically with the fraction of H, as shown in Table 2, presumably because the number of possible cross-link sites is larger. Solutions with lower concentrations of H, such as t-10/0 and t-10/0.5 were also prepared, but these samples were entirely liquid-like, and dynamic frequency sweeps were uninteresting.

To estimate the number of active hydrogen bonds, we previously proposed a simple model for the longest relaxation time of the gel, τ_1, in which relaxation of a network strand requires the simultaneous release of n hydrogen bonds between a single V end block and its H partner. This is determined by a Boltzmann factor involving n times the energy per hydrogen bond, ΔE. This analysis gave

$$n(T) = \frac{T}{T_{ref}} + \frac{RT}{\Delta E} \ln a_T \qquad (1)$$

From FT-IR measurements the energy of a single hydrogen bond was estimated as $\Delta E \approx 13 \pm 2.5$ kJ/mol.[37] With the assumption that $n(T_{ref}) = 1$ near the gel point (130 °C for t-10/2, 140 °C for t-10/4, and 160 °C for t-10/8), $n(T)$ for each sample could be estimated from this equation. The results at room temperature are approximately 4, 5, and 6 hydrogen bonds per V block for t-10/2, t-10/4, and t-10/8, respectively. The estimates of 4 and 6 for t-10/2 and t-10/8 are reasonable numbers compared to 5 for t-10/4 as reported previously,[37] and they indicate that a higher fraction of H induces more effective hydrogen bonds for a given V block and higher gel temperatures. Moreover, these numbers indicate that about 10 mol% of the V repeat units are engaged in hydrogen bonding at the lowest temperatures, which is plausible for the interaction between two short, random coil polymers.

The plots of a_T for the four triblock gel samples displayed in Figure 3 are almost identical, indicating that the longest relaxation times for the triblock samples have the same

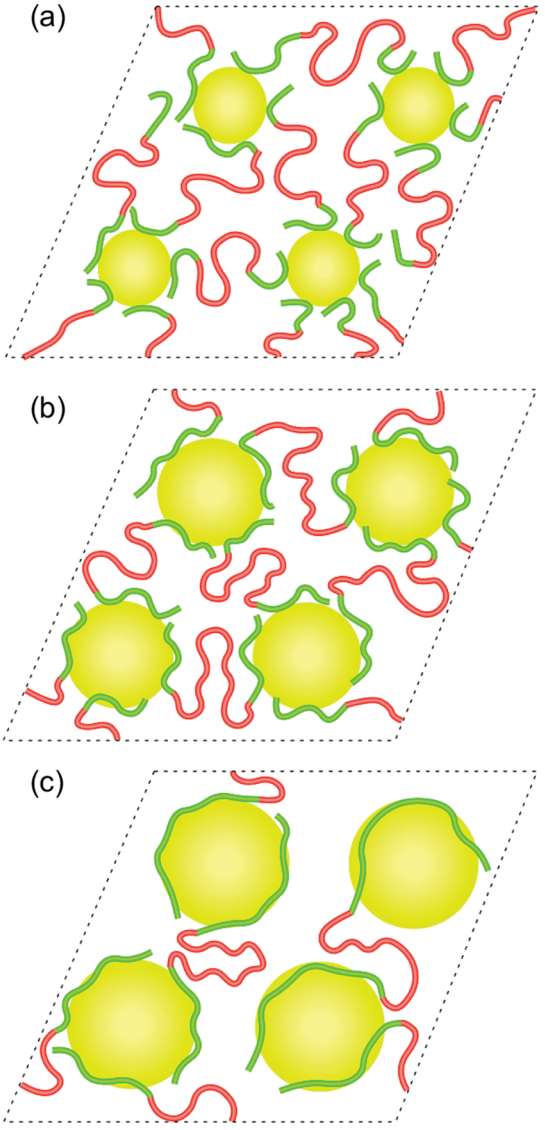

Figure 6. Schematic illustration of association between V blocks (green chains) and H homopolymer (yellow spheres). Red chains represent EA blocks. Cartoons represent (a) t-10/2, with too few phenol units leading to dangling V blocks; (b) t-10/4, with appropriate stoichiometric balance; and (c) t-10/8, with excess phenol units leading to some cross-links with functionality less than 3. For clarity, looping EA chains are omitted from these cartoons.

physical origin. This is consistent with the proposal that the network connectivity is mostly locked in around the gel point, and that on subsequent cooling the main change is an increase in the number of hydrogen bonds, $n(T)$, per V block. It is important to note that a_T, and thus $n(T)$ appear to be saturating at lower temperatures, which establishes that the more than 10 order of magnitude change in τ_1 is not connected to a glass transition.

Quality of the Gels Controlled by Stoichiometric Balance. The gel−liquid transition temperatures increase monotonically with the fraction of H, as shown in Table 2, and the ultimate relaxation mechanism for the triblock samples is equivalent. However, the quality of the resulting gels is not monotonic with H content from Figure 2, but goes through a maximum near t-10/4. In this context we judge the quality of the gel by the magnitude of the plateau modulus, by the sharpness of the liquid to solid transition, and by the minimum value of tan δ in the gel regime. By these criteria, the sample t-10/4 makes the best gel. As illustrated schematically

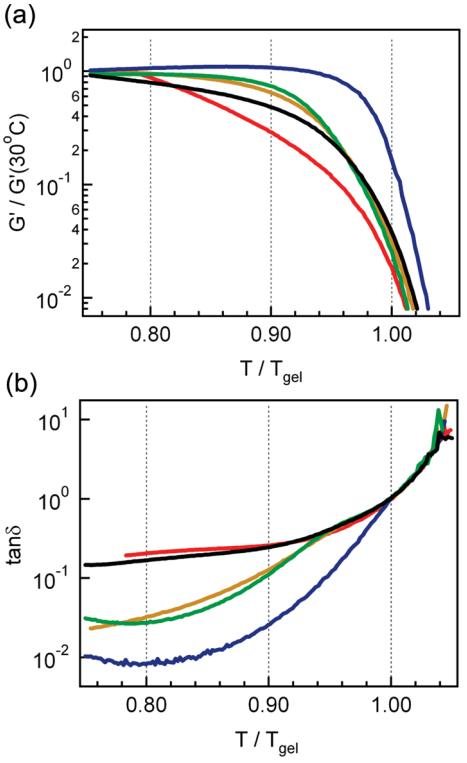

Figure 7. (a) Normalized storage modulus (G'/G'(30 °C)), and (b) loss tangent (tan δ) as a function of normalized absolute temperature (T/T_{gel}). Red curves represent t-10/1, yellow for t-10/2, blue for t-10/4, yellow green for t-10/8, and black for d-10/4. The original data are shown in Figure 1.

in Figure 6b, we attribute this to the stoichiometric balance between hydrogen bond donors (H) and acceptors (V). Thus for t-10/2, the smaller number of phenol units leaves some V blocks unable to locate partners; this results in dangling ends (Figure 6a). At the opposite extreme, an excess of phenol units in t-10/8 generates associations with V blocks that are either "monofunctional" or "difunctional", neither of which creates elastically effective strands (Figure 6c). From Table 2 it appears that the relevant parameter is the ratio of phenol units to pyridine units (as opposed to, for example, the relative number of blocks); for t-10/4 this ratio is 1.6. However, it is not immediately obvious what the ideal ratio should be, given the complexity of the interaction and the topology of network, and the constraints provided by steric hindrance between 2-vinylpyridine and 4-vinylphenol units.

The higher, flatter plateau modulus for t-10/4 may be compared with expectation for an "ideal" gel, for which

$$G_x = \nu k_B T \tag{2}$$

where ν is the number of elastically effective network strands per unit volume. If every EA midblock were elastically effective, then $\nu = cN_A/M$, where $c \approx 0.1$ g/mL, N_A is Avogadro's number, and M is the molecular weight of the triblock copolymer. From the concentration and molecular weight of the triblock, we estimate the maximum possible modulus as 5040 Pa, which is almost exactly twice the observed 2570 Pa. However, it is well-known that ABA triblock copolymers typically loop back into the same micelle at least 50% of the time,[71,72] which would account for the observed modulus. Thus, we may conclude that because of stoichiometric balance, sample t-10/4 provides the best gel that can reasonably be obtained for this triblock molecular weight and concentration.

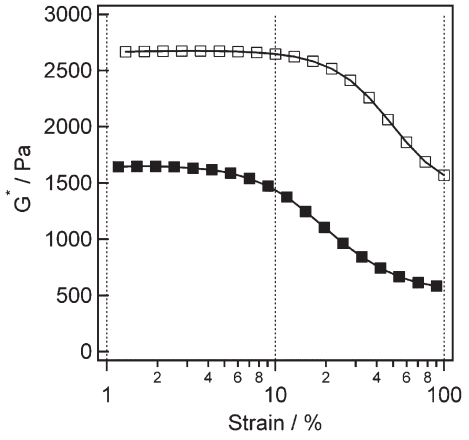

Figure 8. Strain amplitude sweeps for t-10/4 and d-10/4 at 30 °C, where open squares (□) represent t-10/4 and filled squares (■) represent d-10/4. The vertical axis is the magnitude of the complex modulus $G^* = ((G')^2 + (G'')^2)^{1/2}$.

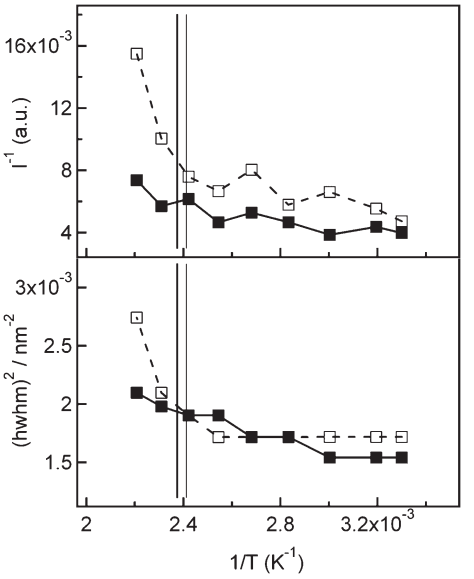

Figure 9. (a) Reciprocal of the maximum of the scattering intensity (I^{-1}), and (b) square of half-width of half-maximum (hwhm)^{2}as a function of inverse absolute temperature. Filled squares represent d-10/4, and open squares for t-10/4. The two vertical lines represent T_{gel}: the line on the left side is for d-10/4 (148 °C) and the other line is for t-10/4 (141 °C).

The relative quality of the gels can also be discerned from Figure 7. Figure 7a shows G' normalized by G' at 30 °C as a function of absolute temperature normalized by the gel point (T/T_{gel}), where the original data come from Figure 1. Figure 7b displays the loss tangent ($\tan\delta = G''/G'$) vs T/T_{gel}. These graphs illustrate clearly how sharply the gels become elastic below T/T_{gel}, and how closely they approach the purely elastic limit. By both measures the t-10/4 gel has a sharper liquid-to-solid transition compared to t-10/2 and t-10/8, which are themselves superior to t-10/1 and d-10/4.

Difference of Relaxation Mechanisms between Triblock Gels and a Diblock Gel. As noted in the Results section, SAXS did not reveal any particular difference between the triblock gels and the diblock gel. However, the rheology data in general, and the shift factors in particular, show significant differences. The four triblock gel samples in Figure 3 show the same dependence for a_T even below 120 °C, but the diblock gel sample is definitely not on the same curve, and in fact the temperature dependence is much weaker. This difference presumably reflects the fact that the gel-like nature of the diblock rheological response comes from congestion of individual "micelles" with V + H cores and EA coronas, rather than from bridging chains. Certainly the weaker temperature dependence is consistent with the idea that the longest relaxation time of the gel sample is not dictated by cooperative release of n hydrogen bonds.

Another way to probe the difference between the triblock and diblock samples is to examine the strain dependence; bridging of triblock copolymer midblocks should be more effective in terms of giving strain robustness. We prepared a sample d-10/1 (VEA/H/IL = 10/1/90) to compare with t-10/1. The mechanical strength of this sample was, in fact, not sufficient to measure, and the sample showed no appreciable viscoelasticity. To pursue this issue more quantitatively, the dynamic strain sweep at 30 °C for t-10/4 is compared with d-10/4 in Figure 8. The diblock gel shows nonlinear viscoelasticity above 4−5% strain, whereas the triblock gel shows linear response up to at least 15% strain. Both of these observations are consistent with the proposed difference between diblock and triblock samples. (See also Figure S17 in Supporting Information.)

Further Discussion

In the previous paper, we inferred that thermoreversibility of the ion gels was not controlled by a classical block copolymer order−disorder transition (ODT),[73−76] but rather by the association−dissociation transition of hydrogen bonding. To understand the relationship between ODT and hydrogen bonding, we analyzed temperature-controlled SAXS for t-10/4 and d-10/4 in more detail as shown in Figure 5. The inverse intensity (I^{-1}) and the square of the half-width of half-maximum (hwhm)^2 of the primary peak for each profile of t-10/4 and d-10/4 are plotted as a function of inverse absolute temperature in Figure 9. Both I^{-1} and (hwhm)^2 for both gel samples decrease gradually, not dramatically, with increase in inversed absolute temperature. In contrast, at the normal ODT temperature (T_{ODT}) there is an abrupt drop in intensity and a substantial broadening of the main peak for block copolymers. Although the symptoms of disordering starts to appear around 140 °C, the peaks at 180 °C still remain sharp as can be seen in Figure 5. Both I^{-1} and (hwhm)^2 gradually increase near the rheological gel points, but never change abruptly. Hence, we may conclude that although nanophase separation is occurring in these solutions, the ODT is not in and of itself the origin of the remarkable gel-like rheological response of the triblock samples with 1% or more added H. It is also important to note that the success of time−temperature superposition both above and below the gel point would not be expected if, in fact, the gel point corresponded to an ODT.

Summary

In this report, we have explored features of a thermoreversible supramacromolecular ion gel system, obtained via hydrogen bonding between a VEAV triblock copolymer with an H homopolymer. The gelation mechanism was clarified by measuring the transition from liquid state to gel state with SAXS and rheology. The gel point (gel−liquid transition temperature) was affected by the concentration of the cross-linkers, *i.e.*, the number of active hydrogen bonding proton donors. Moreover, the best gel was formed at the mole ratio closest to stoichiometry of pyridine and phenol units. It was found that a gel-like response could be obtained by mixing a VEA diblock copolymer and an H homopolymer. However, whereas triblock gels had approximately 50% bridging conformations for the EA midblocks, which leads to an infinite network with hydrogen bonding cross-links, a

diblock "gel" is due to congestion caused by micelles with V+ H cores and swollen EA coronas. Hence, supramacromolecular gelation in an ionic liquid as reported here could also be a useful tool for applications such as actuators, polymer electrolytes, membranes, or gate dielectrics for organic transistors.

Acknowledgment. A.N. thanks JSPS Research Fellowships for Young Scientists (No. 18-6533) and Grant-in-Aid for Young Scientists (B) (No. 21750217) from the Ministry of Education, Culture, Sports and Science, and Technology of Japan. This work was also supported by the National Science Foundation through DMR-0406656 and DMR-0804197 (T.P.L.). The authors also thank Dr. David Giles of the Polymer Characterization Facility, University of Minnesota, for his assistance with the rheology measurements. Use of the synchrotron X-ray source was supported by Photon Factory, KEK in Tsukuba, Japan (No. 2008G187 for A. N.). This work was also partially supported by the Global COE Program in Chemistry entitled "Elucidation and Design of Materials and Molecular Functions", Grant-in-Aid for Scientific Research on Priority Area "Soft Matter Physics" (No. 18068008) from the Ministry of Education, Culture, Sports and Science, and Technology of Japan.

Supporting Information Available: Text giving the details of synthesis and characterization of the polymers, a scheme showing the reactions, figures showing SEC chromatograms, ^{1}H NMR spectra, time−temperature curves, η/η_{303K} and a_T plots, and strain amplitude sweeps. This material is available free of charge via the Internet at http://pubs.acs.org.

References and Notes

(1) Brunsveld, L.; Folmer, B. J. B.; Meijer, E. W.; Sijbesma, R. P. *Chem. Rev.* **2001**, *101*, 4071–4097.
(2) ten Brinke, G.; Ruokolainen, J.; Ikkala, O. *Adv. Polym. Sci.* **2007**, *207*, 113–177.
(3) Berl, V.; Schmutz, M.; Krische, M. J.; Khoury, R. G.; Lehn, J. M. *Chem. Eur. J.* **2002**, *8*, 1227–1244.
(4) Russell, T. P.; Jerome, R.; Charlier, P.; Foucart, M. *Macromolecules* **1988**, *21*, 1709–1717.
(5) Yashima, E.; Matsushima, T.; Okamoto, Y. *J. Am. Chem. Soc.* **1997**, *119*, 6345–6359.
(6) Harada, A.; Kataoka, K. *Science* **1999**, *283*, 65–67.
(7) Hofmeier, H.; Schubert, U. S. *Chem. Soc. Rev.* **2004**, *33*, 373–399.
(8) Frechet, J. M. J. *Science* **1994**, *263*, 1710–1715.
(9) Russell, T. P. *Science* **2002**, *297*, 964–967.
(10) Ober, C. K.; Cheng, S. Z. D.; Hammond, P. T.; Muthukumar, M.; Reichmanis, E.; Wooley, K. L.; Lodge, T. P. *Macromolecules* **2009**, *42*, 465–471.
(11) Cordier, P.; Tournilhac, F.; Soulie-Ziakovic, C.; Leibler, L. *Nature* **2008**, *451*, 977–980.
(12) Beck, J. B.; Rowan, S. J. *J. Am. Chem. Soc.* **2003**, *125*, 13922–13923.
(13) Boal, A. K.; Ilhan, F.; DeRouchey, J. E.; Thurn-Albrecht, T.; Russell, T. P.; Rotello, V. M. *Nature* **2000**, *404*, 746–748.
(14) Yang, X. W.; Hua, F. J.; Yamato, K.; Ruckenstein, E.; Gong, B.; Kim, W.; Ryu, C. Y. *Angew. Chem., Int. Ed.* **2004**, *43*, 6471–6474.
(15) Noro, A.; Nagata, Y.; Takano, A.; Matsushita, Y. *Biomacromolecules* **2006**, *7*, 1696–1699.
(16) Feldman, K. E.; Kade, M. J.; de Greef, T. F. A.; Meijer, E. W.; Kramer, E. J.; Hawker, C. J. *Macromolecules* **2008**, *41*, 4694–4700.
(17) Jiang, S. M.; Gopfert, A.; Abetz, V. *Macromolecules* **2003**, *36*, 6171–6177.
(18) Pispas, S.; Floudas, G.; Pakula, T.; Lieser, G.; Sakellariou, S.; Hadjichristidis, N. *Macromolecules* **2003**, *36*, 759–763.
(19) Asari, T.; Matsuo, S.; Takano, A.; Matsushita, Y. *Macromolecules* **2005**, *38*, 8811–8815.
(20) Kato, T.; Mizoshita, N.; Kishimoto, K. *Angew. Chem., Int. Ed.* **2006**, *45*, 38–68.
(21) Huh, J.; Park, H. J.; Kim, K. H.; Park, C.; Jo, W. H. *Adv. Mater.* **2006**, 18, 624-+.
(22) Matsushita, Y. *Macromolecules* **2007**, *40*, 771–776.
(23) Noro, A.; Tamura, A.; Wakao, S.; Takano, A.; Matsushita, Y. *Macromolecules* **2008**, *41*, 9277–9283.
(24) Tang, C. B.; Lennon, E. M.; Fredrickson, G. H.; Kramer, E. J.; Hawker, C. J. *Science* **2008**, *322*, 429–432.
(25) Pochan, D. J.; Chen, Z. Y.; Cui, H. G.; Hales, K.; Qi, K.; Wooley, K. L. *Science* **2004**, *306*, 94–97.
(26) Dobrosielska, K.; Wakao, S.; Takano, A.; Matsushita, Y. *Macromolecules* **2008**, *41*, 7695–7698.
(27) Muller, M.; Dardin, A.; Seidel, U.; Balsamo, V.; Ivan, B.; Spiess, H. W.; Stadler, R. *Macromolecules* **1996**, *29*, 2577–2583.
(28) Folmer, B. J. B.; Sijbesma, R. P.; Versteegen, R. M.; van der Rijt, J. A. J.; Meijer, E. W. *Adv. Mater.* **2000**, *12*, 874–878.
(29) Yamauchi, K.; Kanomata, A.; Inoue, T.; Long, T. E. *Macromolecules* **2004**, *37*, 3519–3522.
(30) Binder, W. H.; Petraru, L.; Roth, T.; Groh, P. W.; Palfi, V.; Keki, S.; Ivan, B. *Adv. Funct. Mater.* **2007**, *17*, 1317–1326.
(31) Nair, K. P.; Breedveld, V.; Weck, M. *Macromolecules* **2008**, *41*, 3429–3438.
(32) Ge, Z. S.; Hu, J; Huang, M.; Liu, S. Y. *Angew. Chem., Int. Ed.* **2009**, *48*, 1798–1802.
(33) Tanaka, F.; Ishida, M.; Matsuyama, A. *Macromolecules* **1991**, *24*, 5582-5589. 48, 1798−1802.
(34) Tanaka, F.; Edwards, S. F. *Macromolecules* **1992**, *25*, 1516–1523.
(35) Huh, J.; ten Brinke, G. *J. Chem. Phys.* **1998**, *109*, 789–797.
(36) Feng, E. H.; Lee, W. B.; Fredrickson, G. H. *Macromolecules* **2007**, *40*, 693–702.
(37) Noro, A.; Matsushita, Y.; Lodge, T. P. *Macromolecules* **2008**, *41*, 5839–5844.
(38) Mullens, J.; Yperman, J.; Francois, J. P.; Vanpoucke, L. C. *J. Phys. Chem.* **1985**, *89*, 2937–2941.
(39) Ruokolainen, J.; Tanner, J.; Ikkala, O.; ten Brinke, G.; Thomas, E. L. *Macromolecules* **1998**, *31*, 3532–3536.
(40) Dai, J.; Goh, S. H.; Lee, S. Y.; Siow, K. S. *Polym. J.* **1994**, *26*, 905–911.
(41) Welton, T. *Chem. Rev.* **1999**, *99*, 2071–2083.
(42) Sheldon, R. *Chem. Commun.* **2001**, 2399–2407.
(43) Dupont, J.; de Souza, R. F.; Suarez, P. A. Z. *Chem. Rev.* **2002**, *102*, 3667–3691.
(44) Carmichael, A. J.; Haddleton, D. M.; Bon, S. A. F.; Seddon, K. R. *Chem. Commun.* **2000**, 1237–1238.
(45) Harrisson, S.; Mackenzie, S. R.; Haddleton, D. M. *Chem. Commun.* **2002**, 2850–2851.
(46) He, Y.; Li, Z. B.; Simone, P.; Lodge, T. P. *J. Am. Chem. Soc.* **2006**, *128*, 2745–2750.
(47) He, Y.; Lodge, T. P. *J. Am. Chem. Soc.* **2006**, *128*, 12666–12667.
(48) Bai, Z. F.; He, Y.; Lodge, T. P. *Langmuir* **2008**, *24*, 5284–5290.
(49) Bai, Z. F.; He, Y.; Young, N. P.; Lodge, T. P. *Macromolecules* **2008**, *41*, 6615–6617.
(50) Ueki, T.; Watanabe, M. *Macromolecules* **2008**, *41*, 3739–3749.
(51) Lodge, T. P. *Science* **2008**, *321*, 50–51.
(52) Susan, M. A.; Kaneko, T.; Noda, A.; Watanabe, M. *J. Am. Chem. Soc.* **2005**, *127*, 4976–4983.
(53) He, Y.; Lodge, T. P. *Chem. Commun.* **2007**, 2732–2734.
(54) He, Y.; Boswell, P. G.; Buhlmann, P.; Lodge, T. P. *J. Phys. Chem. B* **2007**, *111*, 4645–4652.
(55) He, Y.; Lodge, T. P. *Macromolecules* **2008**, *41*, 167–174.
(56) Jankova, K.; Jannasch, P.; Hvilsted, S. *J. Mater. Chem.* **2004**, *14*, 2902–2908.
(57) Ding, J.; Zhou, D. Z.; Spinks, G.; Wallace, G.; Forsyth, S.; Forsyth, M.; MacFarlane, D. *Chem. Mater.* **2003**, *15*, 2392–2398.
(58) Fukushima, T.; Asaka, K.; Kosaka, A.; Aida, T. *Angew. Chem., Int. Ed.* **2005**, *44*, 2410–2413.
(59) Tang, J. B.; Tang, H. D.; Sun, W. L.; Plancher, H.; Radosz, M.; Shen, Y. Q. *Chem. Commun.* **2005**, 3325–3327.
(60) Lee, J.; Panzer, M. J.; He, Y. Y.; Lodge, T. P.; Frisbie, C. D. *J. Am. Chem. Soc.* **2007**, *129*, 4532.
(61) Cho, J. H.; Lee, J.; Xia, Y.; Kim, B.; He, Y. Y.; Renn, M. J.; Lodge, T. P.; Frisbie, C. D. *Nat. Mater.* **2008**, *7*, 900–906.
(62) Christie, A. M.; Lilley, S. J.; Staunton, E.; Andreev, Y. G.; Bruce, P. G. *Nature* **2005**, *433*, 50–53.
(63) Lai, J. T.; Filla, D.; Shea, R. *Macromolecules* **2002**, *35*, 6754–6756.
(64) Convertine, A. J.; Sumerlin, B. S.; Thomas, D. B.; Lowe, A. B.; McCormick, C. L. *Macromolecules* **2003**, *36*, 4679–4681.
(65) Moad, G.; Rizzardo, E.; Thang, S. H. *Aust. J. Chem.* **2005**, *58*, 379–410.
(66) Lowe, A. B.; McCormick, C. L. *Prog. Polym. Sci.* **2007**, *32*, 283–351.
(67) Noro, A.; Nagata, Y.; Tsukamoto, M.; Hayakawa, Y.; Takano, A.; Matsushita, Y. *Biomacromolecules* **2005**, *6*, 2328–2333.

(68) Bonhote, P.; Dias, A. P.; Papageorgiou, N.; Kalyanasundaram, K.; Gratzel, M. *Inorg. Chem.* **1996**, *35*, 1168–1178.
(69) Noda, A.; Hayamizu, K.; Watanabe, M. *J. Phys. Chem. B* **2001**, *105*, 4603–4610.
(70) Simone, P. M.; Lodge, T. P. *Macromolecules* **2008**, *41*, 1753–1759.
(71) Matsen, M. W.; Schick, M. *Macromolecules* **1994**, *27*, 187–192.
(72) Karatasos, K.; Anastasiadis, S. H.; Pakula, T.; Watanabe, H. *Macromolecules* **2000**, *33*, 523–541.
(73) Leibler, L. *Macromolecules* **1980**, *13*, 1602–1617.
(74) Rosedale, J. H.; Bates, F. S. *Macromolecules* **1990**, *23*, 2329–2338.
(75) Khandpur, A. K.; Forster, S.; Bates, F. S.; Hamley, I. W.; Ryan, A. J.; Bras, W.; Almdal, K.; Mortensen, K. *Macromolecules* **1995**, *28*, 8796–8806.
(76) Ruokolainen, J.; Torkkeli, M.; Serimaa, R.; Komanschek, E.; ten Brinke, G.; Ikkala, O. *Macromolecules* **1997**, *30*, 2002–2007.